CORROSION RESISTANCE OF SUPER AUSTENITIC STAINLESS STEEL IN SEA WATER

By

C. A. Loto* and M. B. Ives,

Institute for Materials Research,
McMaster University, Hamilton, Ontario,
Canada LSS 4M.

ABSTRACT

Field tests and laboratory examinations and analysis have been performed on series of super austenitic stainless steel tubes, of which the inner surfaces were exposed to flowing sea water in a specially designed test rig. The region around the middle portion of the tubes in the test rig was subjected to elevated temperature in the steam chamber part of the rig. The tubes from the field test were examined after splitting in the laboratory with the wild M3C Model optical macro-/microscope and the S.E.M. (Scanning Electron Microscopy). The corrosion deposit and the biofilm were analysed with the S.E.M. equiped with energy Dispersive x-ray (EDAX) spectrometer, and x-ray Diffraction (XRD) spectroscopy. This paper reports the observed corrosion resistance behavior of the tubes' alloys. While all the alloys were found to be generally corrosion resistance in sea water, except the 316L, depending upon the test conditions, they were all also found to be susceptible to crevice corrosion attack at varying degrees under high steam temperature. The crevice corrosion occurred under the strongly adherent calcareous layers deposited in the steam chamber portion of the tubes as observed in one of the runs.

INTRODUCTION

The present interest in the use of super austenitic stainless steel as been brought about by the need to improve the lenght and predictability of service of heat exchangers in chemical industry such as the sulphuric acid manufacture and in condenser tubes at power plants cooled with sea water. These super austenitic stainless steels consist of high chromium, high molybdenum, and often containing nitrogen, silicon and in some cases coper. The 316L used in this work was just for comparison purpose. The recent development of these supper stainless steel alloys has provided better alternatives to the conventional austenitic grades. Because of the high chloride concentration in sea water, the high service temperature, and biofoulding among other factors, stainless steels are susceptible to pitting and crevice corrosion. Chromium and molybdenum contents of stainless steels have been recognised to strongly influence the resistance of stainless steels to localised corrosion. The super stainless steels are those austenitic grades with a minimum of 20% cr and 6% Mo and those ferritic grades with a minimum of 25% cr and 3% Mo.

There has been many literature reviews on pitting corrosion and the effect of alloying elements on reducing it [1,2]. Various models have been proposed. Hoar[3] suggested that molybdenum encourages the formation of an amorphous film which is more protective than a crystalline one. Another more current model suggests the formation of molybdate complex ions in solution which effectively block breakdown sites before it can develop into self-sustaining pits[4].

Several studies have suggested that nitrogen in austenitic stainless steels is also an effective element to improve the resistance to pitting and crevice corrosion[5,6,7]. The most striking effect of nitrogen has been observed in molybdenum bearing stainless steels, suggesting a possible synergism between molybdenum and nitrogen[8,9]. Streicher[10] has also observed that the combined additions of molybdenum, nitrogen and silicon provided effective corrosion resistance behaviour to type 316 stainless steels.

It has been widely reported in the literature[11,12] that metal surfaces immersed in natural or industrial waters undergo a sequence of biological and inorganic changes that lead to biofoulding and passivity respectively[13]. The term biofoulding is commonly employed to differentiate those groups of marine organisms

that grow on artificial structures from those occuring on rocks, stones, and other hard natural surfaces[14]. Its use is frequently limited to situations in which the results of attachment and growth may be considered harmful. Characklis, et al[15] reported that biofoulding leads to an important modification of the metal/solution interface, either partially or totally covered by biofilms and accounts for serious loss of energy in different types of industrial systems. It has been reported[16] that biofilms developing on the heat transfer surfaces of the condenser produce three main effects: increase in fluid frictional resistance; increase in heat transfer, and corrosion. The influence of boifilms on corrosion is determined by the activity at the anodic and cathodic sites[14]. Some of the ways in which biofilm may influence corrosion processes have been outlined[16].

In the super alloy under study, the effects of biofilms on corrosion resistance of the alloys in sea water have not been much documented. However, further work on this is at present under investigation. In this work, corrosion resistance or behavior of different types of super austenitic stainless alloys, in tubes, in which sea water was made to flow through, in a specially designed test rig located at HBOI, Florida, was studied by metallographic electron-optic and spectroscopic methods. The work aims at making a significant contribution to the development of an understanding of the performance and service life of these super austenitic stainless steels in sea water enviroment.

EXPERIMENTAL METHODS

Field Test

Nine tubes, each 2.14 metres long and 19mm dia., made of different alloys of varying chemical composition, - Table 1, were used for the field test. A specially designed test rig located at the HBOI - Harbor Branch Oceanic Institution, Florida, was used for the test running. The tubes were specially fitted in the test rig in such a way as to permit uniform flow of sea water which was being pumped through. There was a steam chamber about 0.205 metres long located in about the middle portion of the tubes length and at which a predetermined steam temperature was maintained. Several test runs were made and each lasting for 60 days averagely. New sets of tubes were used for each test run. The water flow rate varied from one test run to another and it was also being predetermined. Table 2 gives a summary of the field test operating parameters. After each run, the tubes were brought to the laboratory after cutting to some specified lengths, for further examinations and analyses.

Laboratory Examination and Analyses

The cut tubes were each split into two in the laboratory, with the weldment being at one part. The split tubes (already with biofouling) were then cleaned with water, detergent solution and hand brush. In some instances, photographs of the split tubes before and after cleaning were taken before further examination with the Wild M3C Model Optical macro-/microscope. This macroscope was used to observe the whole length surface of each tube to locate the occurrence or site of any pit or local corrosion attack sites. Visual observation was also used for the visually visible corrosion sites. Some of the microscopic corrosion pits' micrographs were taken with the Scanning electron microscopy (S.E.M.).

Biofil/Corrosion Deposit Composition Analyses

Some of the cut ring samples, with the inner tube surface biofilms - specifically, the tubes made of 904L and 316L alloys from the stream chamber and the outlet portions, of two different test runs, were dried (dehydrated) in an oven at 100°C for 4 hours after the distilled water and acetone cleaning. The specimens were each split into two and their surface biofilm composition analysed with the EDAX (Energy Dispersive X-ray) spectroscopy. The specimens used for the analysis were randomly selected. Further analysis was performed on the corrosion deposit, steam chamber's portion biofilm and the tube's outlet biofilm's composition using the X-ray Diffraction (XRD) technique and the EDAX. This was done on a selected tube, made of AL6XN alloy, that was used in two consecutive runs. This tube experienced variable operating parameters for a total of 120 days.

RESULTS

Visual, Metallographic and S.E.M. Examinations

The biofilm on the inner surface of all the tubes, in general, was slightly thick but easily removed with hand brush and water. The biofilm in the steam chamber portion was either very light, non-existent or with strong adherent calcareous deposit as observed in one of the test

runs.

The super austentic stainless steels were generally very corrosion resistant. The 316L used along with them was not corrosion resistant. It failed visibly in all the test runs. It was used for comparison purpose. All the other steel alloys corroded slightly with very little microscopic pits in the steam chamber and the stream outlet. Quite a number of microscopic pits or sites of local corrosion attack were obtained along the weldment of the tubes made with AL6XN alloy in all the test runs. Most of the corrosion attack observed were not deep penetrating. They were shallow, flat, and some roundish, Fig. 1.

The biofilm covering the inside surface of the tubes for one of the test runs was quite different. The striking differences was more noticeable in the steam chamber portions. The biofilm was very strongly adherent to the metal surface for all the tubes. Brush and soap solution could not remove this. It had to be scraped with the other metallic and handle of the brush used. Located under the adherent biofilm, were different forms of corrosion attack; and were mainly microscopic, Fig. 2. A summary of this result is presented in Figure 3. All the tubes had corrosion attack under the deposit but to varying degrees. Figures 4-7 are further indications of the corrosion attack on some of the tubes. The least corrosion attack occurred in the tubes made of 254 SMO (S31254) alloy and closely followed by those made of 1925 HMO (N08925) alloy. The corrosion attack concentrated mainly in the steam chamber portion.

EDAX Spectroscopy Analysis

The EDAX spectroscopy analysis results showed the presence of many chemical elements as presented, for example, in Figures 8-12. The biofilm collected from the steam chamber portion of the tube made of 940L (N08904) alloy, Fig. 8, consists of Ca and P in addition to Fe, Cr and Ni. The tube's outlet biofilm appears to consist more of Fe, Si, and Cr. The steam chamber's portion biofilm, of the tube made of 316L alloy, Figure 9, consists of Si, Mg, P, Cl, and Ca among others. The tube's outlet biofilm consists more of Si, P, Al and Ca in descending order, Fig. 10.

The corrosion deposit taken from a macroscopic pit in one of the tubes made of AL6XN, (NO8367), consists relatively more proportion of Fe, Cr, Si and Ca, Fig. 11. The presence of S and Mo is very difficult to ascertain as both share the same signal. The two elements would likely be present together. The tube's outlet portion biofilm consists more of Si, Cl, Ca and Fe in descending order. Ca was more predominant in the biofilm obtained from the steam chamber portion of the same tube, Fig. 12. This was followed by the presence of Si, Mg, and Fe. The biofilm in the steam chamber was very adherent to the tube's inner surface.

X-ray Diffraction Analysis

The results obtained from the x-ray diffraction analysis of the corrosion deposit obtained from a pit located at the steam chamber's portion of one of the tubes made of AL6XN (NO8367) alloy, and the biofilm from the steam chamber and the outlet portions of the tube are presented in Figures 13-15. The corrosion deposit consists of many phases of which the major ones are Fe_2O_3, (Fe_3O_4) $Fe(CrO_4)OH$; and amorphous materials (substantial amount). Different phases were also present in the tube's steam chamber portion biofilm of which the major phases are: $Ca_4(SiO_3)_3(OH)_2$; calcite and aragonite - $CaCO_3$; spinel - MgO - like structure materials. The biofilm from the tube's outlet portion consists of: NaCl as the major crystalline material; $CaCO_3$; very small amounts of FeOOH; and other crystalline and amorphous materials.

DISCUSSION

The over-all results obtained, as presented earlier in this paper suggest that all the alloys are relatively corrosion resistant under the testing condition (Table 2) except the 316L which was generally non-corrosion resistant in sea water throughout the testing period. Though tested with other super austenitic stainless steel, 316L (S31603) alloy does not actually belong to this category of steels because of its relatively lower Mo content. The general statement above, about the relative corrosion resistance of the alloys, does not, however, hold under some particular testing condition(s). This assertion could be indicated with a situation whereby a strong adherent calcareous layer deposit occurred as observed in one of the test runs in this work being reported. It led to under deposit corrosion in the steam chamber portion of all the steel tubes tested, though to varying degrees.

In general, the corrosion attack resistance of all the alloys tested, except the 316L, was due

to the very high alloying contents of the steels - particularly the Mo, Cr, Ni, N and to some extent Si and Mn. As earlier mentioned, these metallic elements have been known[1-9] as providing stable passivity for the corrosion resistance of these alloys in corroding media. The high Mo content, in particular, has been found to have very high and stable passivating effect[1-4]. However, the slight differences observed in the magnitude of their corrosion resistance capability, could be due, among others, to the influence of their variable metallurgical compositions and/or their surface finishing characteristics as presented in Table 1, and exemplified in Figs. 16 and 17 respectively.

The significant observation in this work is that substantial crevice corrosion attack occurred in the steam chamber portion of the tubes when there was strong adherent calcareous layer deposit. This situation was observed only once throughout the whole test runs made. Even when crevice condition was designed into some of the tubes, crevice corrosion attack occurred conspicuously at the longitudinal end of one of the tested tubes - 1925 HMO. The situation that has made the calcareous deposit possible is very difficult to explain precisely. This was because most of the test runs were carried out under similar operating conditions; though some with intentional and unintentional variations. An attempt to reproduce the strong, adherent and slightly thick calcareous deposit on the metal surface did not succeed. This might be due to unavoidable irregularity and anomaly of some inconsistent stoppages caused by power failures among others during the tests.

The tests were performed during different periods of the year: The seasonal variation could influence the amounts of dissolved ions/chemicals in the sea water, especially the calcium carbonate and magnesium carbonate/sulphate species[17]. These situations could account, in part, for the different results obtained from one test run to another.

The problem created by the operating anomaly (such as stoppages), in the steam operating conditions could affect the non-uniformity of results; particularly with respect to calcareous deposition. The test rig operating conditions, with its elevated temperature at the steam chamber portion of the tubes could disturb the balance between the calcium compounds and CO_2 in the sea water used. This type of situation has been known to promote abnormal deposition of calcium carbonate on metal surfaces[18]. The strong adherence to the metal surface could be due to the high tube wall temperature. The high steam operating temperature would cause further precipitation of the $CaCO_3$, $MgCO_3$, and $Mg(OH)_2$ etc. in the sea water flowing through the steam chamber[19]. Their solubility decreases with increasing temperature.

Deposition of calcareous layers is enhanced by increase in pH of the sea water[20-24]. The high steam temperature did not only disturb the calcium compounds and CO_2 balance of the sea water, but also caused oxygen depletion within the steam chamber portion of the tested steels. The later phenomenon would not only cause less passivity to the steel alloys but also increased the sea water alkalinity - increase in pH, with the consequential calcareous deposition which were mainly calcite and aragonite as confirmed by the x-ray diffraction analysis. Bacteria were not detected at the steam chamber section of any of the tubes where under-deposit corrosion attack occurred, and could not therefore be considered here.

The condition under the calcareous layer would be that of severe oxygen depletion; and increased alkalinity - pH at the metal-electrolyte (sea water) interface. This in combination with the high chloride ions from the sea water, and the carbonate and sulphate ions, would cause the depassivation of the tube's metal passive film. As a result, anodic and cathodic corrosion sites were created leading to anodic and cathodic corrosion reactions. Crevice corrosion then occurred by the metal's anodic dissolution under the deposits. The corrosion reaction kinetics was likely aided by the elevated temperature used.

Mechanistically, the over-all corrosion process must be that of synergism among the various factors involved; and crevice condition(s) must be available before any reasonable corrosion attack (crevice) could occur.

The EDAX spectroscopy analysis, (Figures 8-12), confirms the tubes' surface biofilm enrichment at the different areas of the tubes as consisting of different chemical elements. These include Ca, Mg, Cl, P, and Si. The particular effect of these chemical elements on the biofilm structure, corrosion characteristics, biofilm properties and hence on the corrosion of the tube metal alloys is not yet very clear. However, while chloride ions (Cl) would make a significant contribution towards the depassivation of the

alloys' protective film, others such as Cr, Ni, Mo, Mg and Si were presumably giving some beneficial effects of stabilising the alloys protective film; while at the same time prevent the biofilm's growth that could lead to increased corrosion among other adverse effects.

The x-ray diffraction analysis confirms that the biofilm in the steam chamber was more enriched with Fe, Ca, and Mg than the outlet biofilm. It further confirmed the presence of $CaCO_3$ - calcite and aragonite, as the major composition of the calcareous layer deposited on the metal's surface which provided suitable crevice condition for corrosion attack.

CONCLUSION

1. All the super austentic stainless steels gave general impressive corrosion resistance in sea water except under crevice environment test conditions.

2. The 316L alloy, albeit not super stainless steel, was susceptible to pitting and crevice corrosion attack in sea water under all the testing conditions but more at elevated temperature(s) in the steam chamber.

3. All the alloys were susceptible to crevice corrosion attack but at varying degrees. Any condition that could create crevice environment during the use of these super austentic stainless steels (in sea water) must be avoided.

4. Alloys 254 SMO (S31254) and 1925 HMO (NO8925) showed superior corrosion resistance relatively.

5. The role of the chemical elements and compounds within the biofilm matrix is not yet very clear, but some such as Cr, Ni, Mg, Mo, and Si, seem to contribute to stabilising the protective passive films on the metal alloy surface. Others such as $CaCO_3$, $MgCO_3$, - sulphates and hydroxides form the major constituent of the calcareous deposition and created crevice condition(s) on the metal surface for crevice corrosion attack. Calcareous deposition is definitely not good for these alloys in sea water.

ACKNOWLEDGEMENTS

This work was supported by grants from Chemetics International Company Ltd; The University Research Incentive Fund (Province of Ontario), and the Natural Sciences and Engineering Research Council of Canada.

REFERENCES

1. A.J. Sedriks, "Corrosion of stainless steels", Wiley Intersci., 1979, pp.70-74.

2. Z. Skzlarska-Smialowska, "Pitting Corrosion of Metals", NACE, 1986, PP. 145-156.

3. T.P. Hoar, J. Eletroch. Soc. 117, p.170, (1970).

4. J.R. Ambrose, Corrosion, 34, p. 27, (1977).

5. J.E. Truman, M.J. Coleman, K.R. Pirt, Brit. Corr. J. 12, 236, (1977).

6. J. Eckenrod, C.W. Kovack, ASTM STP 679, pp.17, (Philadeiphia, PA, 1977).

7. K. Osozawa, N.Okato, in "Passivity and its Breakdown on Iron and Iron Based Alloys", NACE, Houston, TX 1976, pp. 135.

8. R. Bandy, D. Van Rooyen, Corrosion, 39, 227, (1983).

9. A.J. Sedriks, Intl. Metal, Reviews 28, 306, (1983).

10. M.A. Streicher, J. Electrochem. Soc. 103, 375 (1956).

11. W.G. Characklis, Biotech. Bioeng. 23, 1923-1960, (1981).

12. J.W. Costerton, G.G. Geesey and K.J. Cheng, Sci. Amer. 238, 86-95, (1978).

13. H.A. Videla, in "Structure and Function of Biofilms" eds. W.G. Characklis and P.A. Wilderer, Chichester, U.K. (John Wiley & Sons Ltd). pp.301-320, 1989a.

14. G.J. Brankevich, M.L.F. de Mele and H.A. Videla, MTS J., 24, 3, pp.8, (1990).

15. W.G. Characklis, B.J. Little and M.S. McCaughey, 'Biofilms and their effect on local chemistry, EPRI Workshop on Microbial Induced Corrosion, Charlotte, North Carolina, pp.47, (1988).

16. W.G. Characklis and K.E. Cooksey, Advances in Applied Microbiology, 29, 93-138, (1983).

17. R.H. Heidersbach (Chairman), "Marine Corrosion", Metals Handbook, pp.894, ASM International (1987). Ninth edition.

18. F.L. Laque, Marine Corrosion, pp.95-112, John Wiley & Sons, (1975).

19. S.H. Lin and S.C. Dexter, Corrosion J., 44,9, Sept., pp.615-622, (1988).

20. K.G. Compton, Proc. Int. Corr. Forum, Toronto, 1975, NACE, Paper 13.

21. R.A. Humble, Corrosion J., 4,7, pp.358-370, (1948).

22 E J Zeller and J.L. Wray, Bull. Amer. Assoc. Petro. Geog., 40,1, pp.140-152.

23 S.L. Wolfson and W.H. Hart, Corrosion J., 37,2, pp.70-76, (1981).

24. P.O. Gartland, E. Bardal, R.E. Andresen and R. Johnsen, Corr. J., 40,3, pp.127-133, (1984).

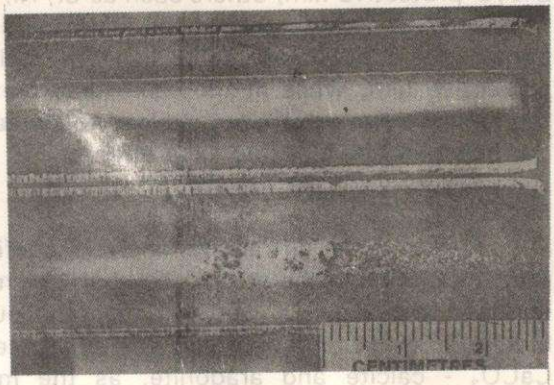
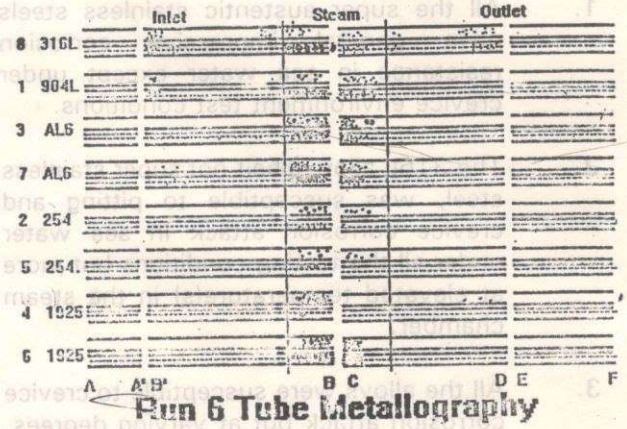


Fig. 2



Run 6 Tube Metallography

Fig. 3



Fig. 1

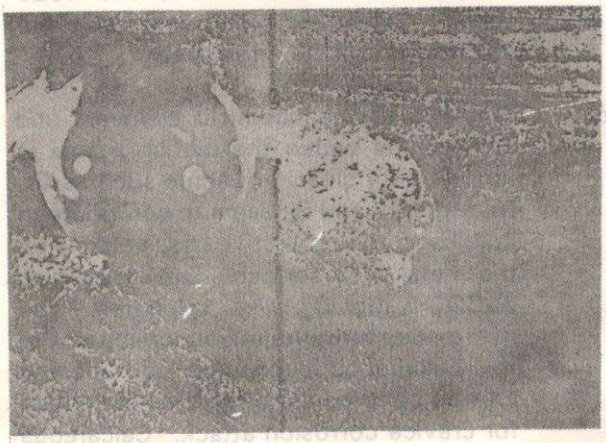


Fig. 4

TABLE 1

CHEMICAL COMPOSITION OF SUPER AUSTENITIC STAINLESS STEELS

Tube No	Alloy/UNS	ELEMENT % Cr	Ni	Mo	Cu	Mn	c	P	S	Si	N
1	904L(N08904)	19.0-23	25.0	4.5	1.5	2.0	0.02	.045	.035	1.0	-
2&5	254SMO (S31254)	19.5-20.5	18.0	6.25	1.0	1.0	0.02	0.03	.01	.80	.20
3&7	AL6XN (N08367)	20.0-22	24.5	6.5	-	2.0	0.03	0.04	.03	1.0	.23
4&6	1925HMO (N08925)	24.0-26	20.0	6.5	1.0	1.0	0.02	0.045	.03	0.5	0.20
8	316L(S31603)	16-18	10-14	2-3	-	2.0	0.03	0.045	.03	1.0	-
9	Dummy	(Any of the above - as specified).									

TABLE 2

TEST CONDITIONS

Run #	Days	Steam Temp.(°C)	Water flow rate (ft/s)
4	59	140-160	4.5
5	64	162	4.5
6	61	160	9
7	60	130	1
8	61	160	9

LIST AND LEGENDS FOR THE FIGURES

FIGS. **LEGENDS**

1. S.E.M. Micrograph of local corrosion attack on the inner surface of 1925HMO (NO8925) alloy tube.

2. Optical macrograph of under deposit corrosion on the inner surface of some of the split tested tubes.

3. Schematic diagrams showing the locations and extent of corrosion in all the tested tubes (except the dummy) in one of the test runs where there was adherent calcareous deposit.

4. Optical macroscope (Wild M3C Model) photograph of an under deposit local corrosion attack site in 904L alloy tube. Mag.x 10. (Glass ball size = 2.5mm).

5. Optical macroscope photograph of an under deposit local corrosion attack site in AL6XN (NO8367) alloy tube. Mag.x 6.4 (Glass ball size = 2.5mm).

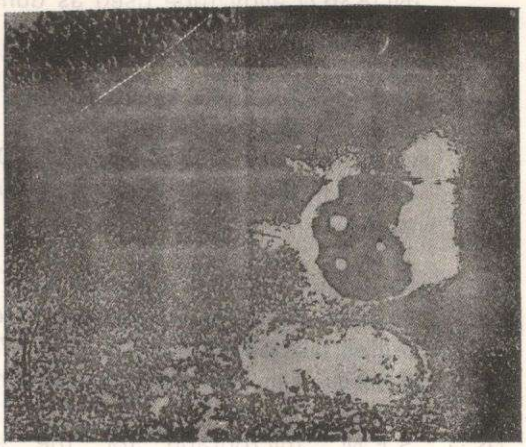


Fig. 5

6. Optical macroscope photograph of other numerous under deposit local corrosion attack site in AL6XN (NO8367) alloy tube. Mag.x 6.4 (Glass ball size = 2.5mm).

7. Optical macroscope photograph of an under deposit local corrosion attack site in AL6XN (NO8367) alloy tube. Mag.x 6.4 (Glass ball size = 2.5mm).

8. EDAX analysis of the biofilm in the steam chamber portion of 904L (NO8904) alloy tube.

9. EDAX analysis of the biofilm in the steam chamber portion of 904L (NO8904) alloy tube.

10. EDAX analysis of the biofilm in the outlet portion of 316L (S31603) alloy tube.

11. EDAX analysis of the corrosion deposit obtained from a macroscopic local corrosion attack site in the steam chamber portion of AL6XN (NO8367) alloy tube used as dummy in two test runs.

12. EDAX analysis of the biofilm from the steam chamber portion of AL6XN (NO8367) alloy tube used as dummy in two test runs.

13. X-ray diffraction (XRD) spectroscopy analysis of the corrosion deposit from a macroscopic local corrosion attack site in the steam chamber portion of AL6XN (NO8367) alloy tube used as dummy in two test runs.

14. X-ray diffraction spectroscopy (XRD) analysis of the biofilm from the steam chamber of portion of AL6XN (NO8367) alloy tube used as dummy in two test runs.

15. X-ray diffraction spectroscopy (XRD) analysis of the biofilm obtained from the outlet portion of AL6XN (08367) alloy tube used as dummy in two test runs.

16 S.E.M. micrograph for the surface characterisation of 254 SMO (S31254) alloy tube used in the sea water test.

17 S.E.M. micrograph for the surface characterisation of 1925 HMO (NO8925) alloy tube used in the sea water test.

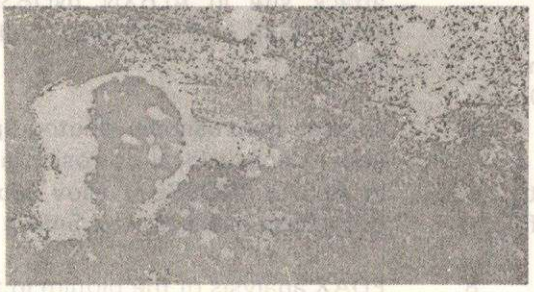


Fig 6



Fig. 7

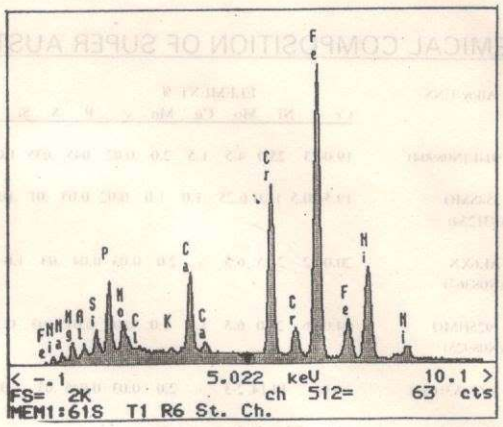


Fig. 8

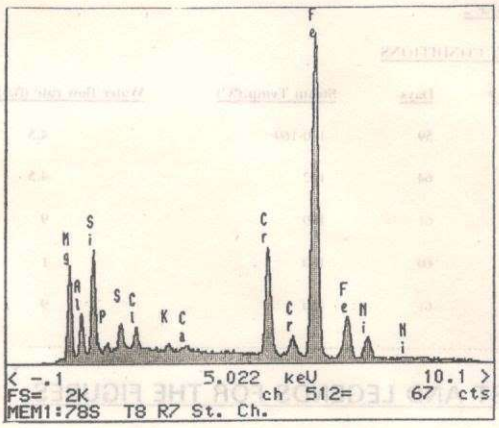


Fig. 9

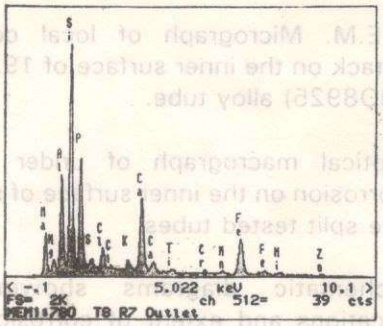


Fig. 10

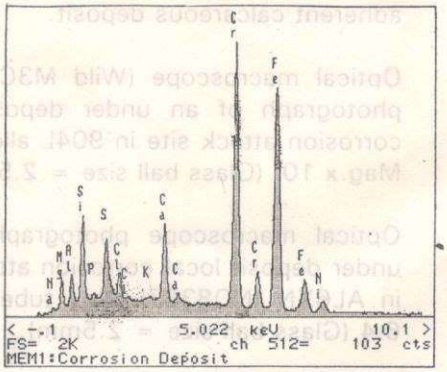


Fig. 11

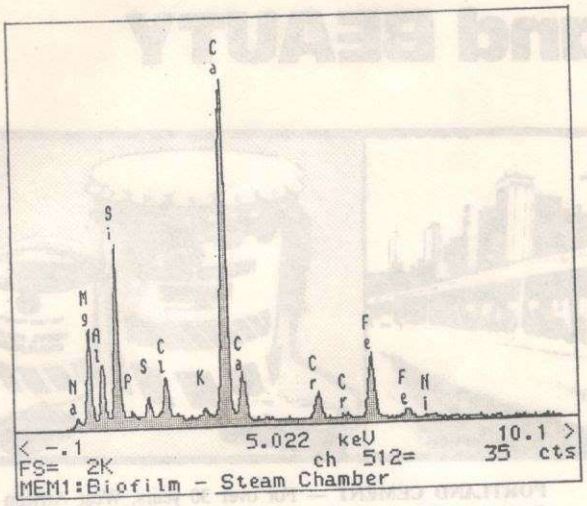


Fig.12

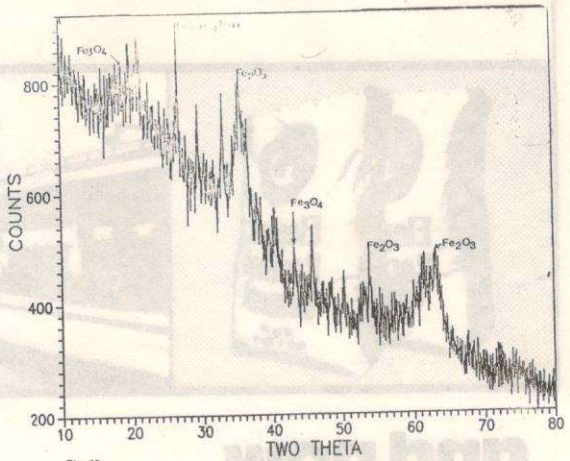


Fig.13

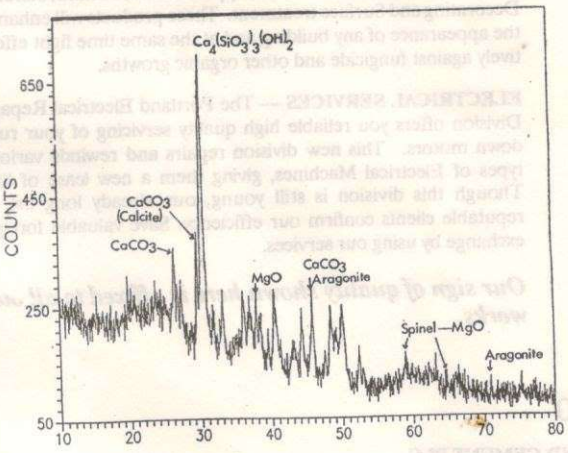


Fig 14

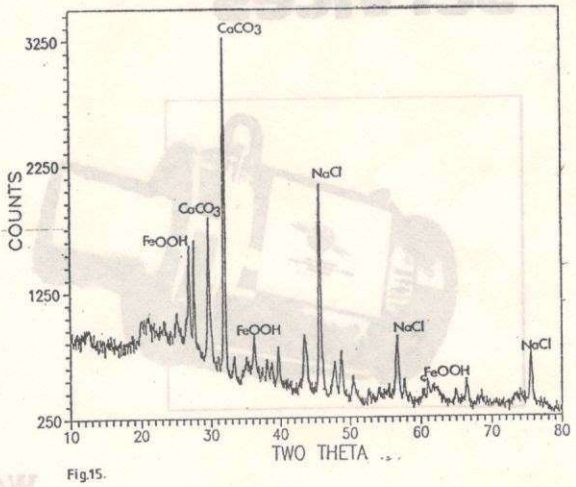


Fig.15.